Chapter 3
Aramid Polycarbonate Resin Film Engineered Composite for Ballistic Protection: Engineered Layered Materials

Ramdayal Yadav, Minoo Naebe, Xungai Wang, and Balasubramanian Kandasubramanian

1 Introduction

The modern battlefield involves threats not only from the enemy combatants but also includes continuous friction and low-velocity impact hazards from the civilian populace, and it is intensified as conflict matures [14]. Carr et al. have reported that such a dynamic state of circumstances in the battlefield renders major causalities due to the generation of lethal fragments compare to those caused by a bullet [14]. The importance of protection was realized through the outnumbered causalities during World War I and various other conflicts around the world [77]. In the recent years, the new avenue of materials has been extensively exploited based on natural armor design strategies imitating the interdigitating hierarchal structures of natural species like mollusk shells, lotus leaves, spider silk, etc. These structures are exploited due to their multifunctional ability and high mechanical properties compared to their constituent material composition, lightweight, and multi-hit capabilities. [4, 23]. Though, a number of such natural structures have been studied extensively but imitating those hierarchies in synthetic materials at a various length scale are yet to achieve. However, among various reported studies on natural architecture, layer by layer assembly of nacreous structure has been widely explored due to their high mechanical properties like high strength as well as high toughness in addition to their multi-hit capabilities. Mollusk shells are regarded as layered structure with calcite (rhombohedral) or aragonite (orthorhombic) (95–99%) and organic materials (0.1–5%) like proteins and polysaccharides [34].

R. Yadav · M. Naebe · X. Wang
Institute for Frontier Materials (IFM), Deakin University, Melbourne, Australia

B. Kandasubramanian (✉)
Defence Institute of Advanced Technology, Deemed University (DU), Ministry of Defence, Pune, India
e-mail: meetkbs@gmail.com

S. Sahoo (ed.), *Recent Advances in Layered Materials and Structures*,
Materials Horizons: From Nature to Nanomaterials,
https://doi.org/10.1007/978-981-33-4550-8_3

Though various materials and combination of the process were exploited to biologically mimicking the hierarchical architecture of nacre and its emulation in commercially available systems have been least reported. In recent years, fiber-reinforced composites have been extensively exploited for the development of efficient ballistic material due to their high strength, stiffness, and specific strength [3]. The ballistic response of fiber-reinforced composite utilizes thermoset and thermoplastic as a polymer matrix. Though thermoset has demonstrated superior tensile, shear, and compressive strength but low-temperature storage, hot/wet stability, and long curing process curtails its exploitation as fiber-reinforced polymer matrix [9, 15–17]. In the recent years, thermoplastic are preferred widely as matrix over thermoset due to their ability to recycle, relatively easy processing into different shapes and sizes as well as long shelf life [45, 69]. Apart from thermoplastic, a number of fibers have been employed for the development of ballistic composite including E-Glass, S-Glass, aramid (Kevlar®-29,49, 129), Nylon 66, poly (p-phenylene benzobisoxazole) (Zylon®), etc. [19, 36, 76]. Among all the class of lightweight fibrous materials, aramid fiber has been gleaned as a prominent example of laboratory experimentation to commercialization. Aramid fiber is a long polymer chain of poly-paraphenylene teraphthalamide that exhibits extraordinary mechanical properties like high strength to weight ratio, high modulus, and toughness with excellent dimensional stability [31, 47, 67].

In the current study, we have demonstrated the utilization of resin transfer molding technique (resin-fiber-infused technique) for fabricating high-performance reinforced polycarbonate composite to mimic the natural nacreous design strategies. Though, various combinations of thermoplastic and high-performance fiber have been exploited [3, 8, 25, 26, 28, 68], but the elucidation of polycarbonate for ordinance velocity range has been least reported in the context of layered natural armor exoskeleton. In addition to ballistic efficacy, we have also discerned the thermal attribute of developed composite and demonstrated that fiber reinforcement had eclipsed the thermal characteristics of polycarbonate in addition to its mechanical property (impact characteristic). The thermal stability of the composite was also evaluated on the basis of the linear approximation of Arrhenius equation at the onset temperature of degradation and in the region of degradation.

2 Materials and Experimental Details

Polycarbonate (PC) (MFI = 10.5 g/10 min, viscosity 22 cp, LEXAN grade 143R) was purchased from SABIC Innovative Plastics India Pvt Ltd, India. Aramid fiber was obtained from the Naval Materials Research Laboratory (NMRL), DRDO, Ambernath, India. The composite was fabricated via a resin-fiber-infusion technique, as illustrated in Fig. 1 [59]. The fabrication method includes transferring the desired dimension of polycarbonate at aramid fabric (placed over metallic mold plate), ensuring proper interaction between fabric and polycarbonate film. This process was further repeated until the required dimension and thickness is not achieved. The

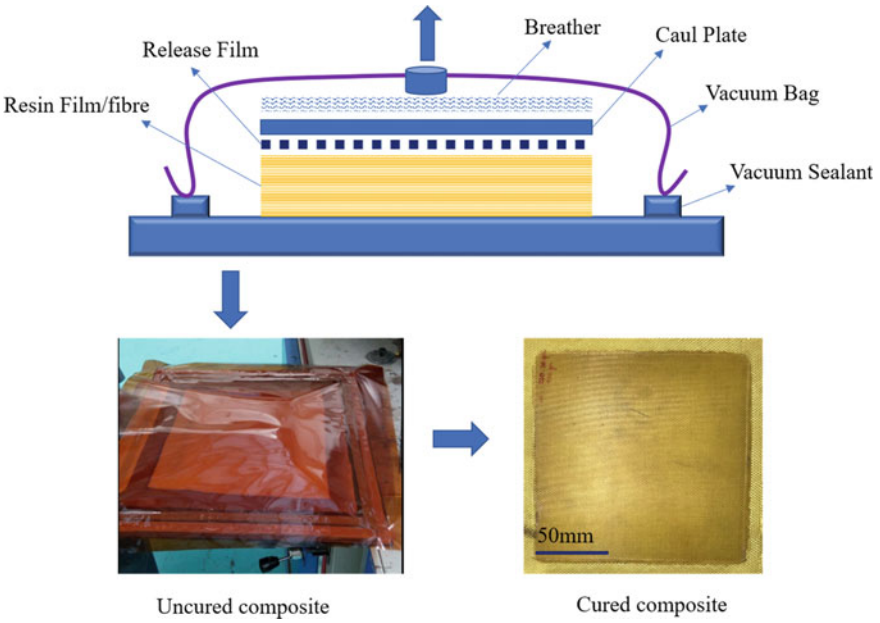

Fig. 1 Processing technique for fiber-reinforced layered polycarbonate composite (FRL PC composite)

layered stacks were placed inside the vacuum bag, as illustrated in Fig. 1, followed by the increasing temperature at 2°C/min till 285°C (melting temperature of polycarbonate). The layered stacks of polycarbonate and aramid have been allowed to be held until the complete infusion is not achieved (the time was optimized for 20 min). The curing process was performed in the oven followed cooling to room temperature before demolding [7]. The standard operating procedure utilized in the current study has been provided in Table 1. The impact property of developed composites was conducted as per ASTM standard D256, while thermomechanical properties were evaluated by dynamic mechanical analysis (TA Q800-USA) under the condition 2

Table 1 Standard operating procedure for developing polycarbonate layered composite

Conditions	Operations
Reinforcement	Aramid fiber (223GSM)
Matrix	Polycarbonate (250GSM)
Required dimension	150 mm × 150mm
Targeted fiber volume fraction	57%
Weight of uncured composite	218.72 g
Curing condition	Ramp from ambient to 285 °C at the rate of 5 °C/min
Dwell time	20 min at 285 °C

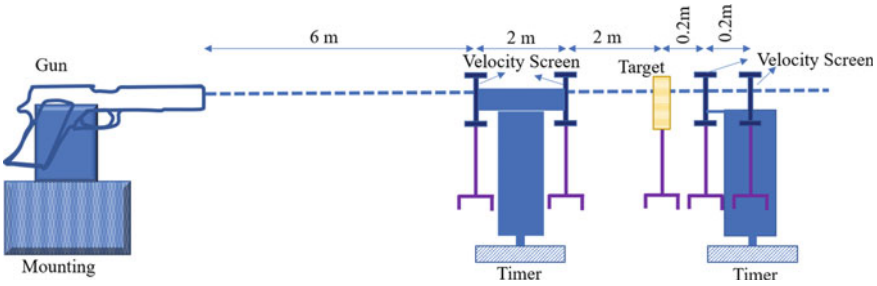

Fig. 2 Ballistic test setup

°C/min heating rate from room temperature to 200 °C. Thermal properties of developed layered composites have been evaluated by differential scanning calorimetry in addition to temperature modulated conditions (TA Q200-USA). Thermal gravimetric analysis was also conducted to understand the degradation phenomenon (TA Q50-USA. Field emission scanning electron (FESEM) microscope was utilized to conduct the fracture surface analysis for the samples (FESEM, Carl-Zeiss, Germany).

2.1 Ballistic Experiment

Ballistic efficacy of layered polycarbonate/aramid composite was assessed by inhouse small arm ballistic facility of Defence Metallurgical Research Laboratory, DRDO, Kanchanbagh Hyderabad, India as elucidated in Fig. 2. 7.62 × 39 mm mild steel core projectile was fired at the distance of 10 m from the muzzle end of the gun [60].

3 Results and Discussion

The development of nacreous structure in nature is a slow process and involves the absorption of minerals and organic matter for intermittent deposition in brick and mortar architecture [18, 49]. The imitation of such slow growth process with analogous environmental stimulus in laboratory is not apparent, but the extensive effort has been employed to mimic natural exoskeleton in artificial materials [65, 66, 71–74, 81]. Self-assembly and sequential deposition are widely exploited methodology for developing a natural armor system in artificial materials in terms of nano and micro-dimensionality. Yao et al. have reported the vacuum filtration or water evaporation technique to mimic the nacreous structure in chitosan and montmorillonite bionanocomposite film [79]. They have demonstrated that the incorporation of nacreous architecture in hybrid building block has rendered augmented

Young's modulus and ultimate tensile strength in addition to enhanced fire retardancy. In another study, Cheng et al. have demonstrated the cross-linking of two-dimensional graphene oxide sheets with π-conjugated long-chain polymers made of 10,12-pentacosadiyn-1-ol (PCDO) monomers via a conjugated cross-linking method. Graphene oxide sheets in this study have been considered as a brick, while PCDO is gleaned from being a mortar phase in artificial nacre [20]. The developed composite avails comparable organic content to the natural nacre in the composite in addition to the distinct organic and inorganic phase with excellent tensile and toughness.

It has been observed that most of the work mainly focuses on an emulation of analogous mollusk architecture at nano or micro-dimension, but we have demonstrated that even macroscopic mimicking of such structure possesses the ability to demonstrate enhanced mechanical property [75]. In this abstraction, we have demonstrated the hypothesis of mollusk layered assembly architecture where polycarbonate has been considered as a soft organic phase, while aramid fiber is contemplated as a hard rick structure. The macroscopic exoskeleton of developed composite layered fiber-reinforced composite has been elucidated in Fig. 3 a–d. Figure 3b delineates the intact layered architecture analogous to the nacreous structure reported by Yao et al. and Cheng et al. in the previously elaborated study, while Fig. 3c renders intermittent alternative assembly of polycarbonate and aramid fiber. The thermal and mechanical

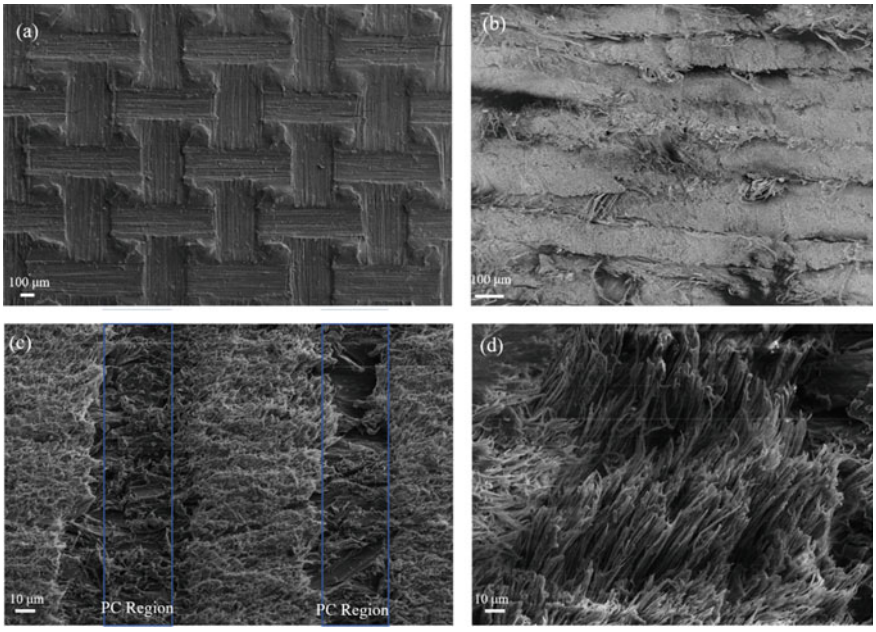

Fig. 3 Layered assembly of polycarbonate and aramid fiber **a** top view of the composite, **b** cross-sectional view, **c** cross-sectional view at higher magnification, and **d** cross-section view of reinforced fiber

property of the developed composite has been elaborated in a later section in addition to the ballistic efficacy against high-speed muzzle velocity.

Polycarbonate has been considered as a prominent commercially available amorphous polymer due to its high toughness and impact resistance [28, 39] and exhibits nearly all mechanical attributes of the glassy polymer at the different combination of time and temperature [80]. The characteristics of polycarbonate have been explored by number of methodology including dynamic mechanical analysis [74, 80], positron lifetime spectroscopy [44], dielectric [53] and nuclear magnetic spectroscopy [54]. Among various reported techniques, dynamic mechanical analysis has been observed to be the prominent technique which possesses the ability to resolve elastic and viscous component of polymer [64]. Dynamic mechanical analysis of polycarbonate was studied by Illers et al. at 1 Hz frequency from torsional pendulum reported three relaxation peaks at +155, +80 and −97 °C, subsequently corroborated as α, β, and γ, respectively [40, 80].

Among these three relaxations, α transition is enumerated to the glass transition temperature, while β transition is related to the small localized chain motion or processing condition [29, 37]. γ transition in polycarbonate is a debatable point and extensively deliberated by Yee et al. [80]. In the current study, we are mainly concentrated on structural and impact application of the developed composite; therefore, the relaxation related to the glass transition is primarily focused. Figure 4a–c and d–f elucidated the dynamic mechanical analysis of pristine polycarbonate and FRL PC composite, evaluated by tensile and 3-point bend test, respectively. As delineated in Fig. 4b–c and e–f, the storage (elastic component) and loss modulus (viscous component) were observed to be augmented in FRL PC composite. In our previous study, we have demonstrated that the peak of Tan δ (ratio of loss modulus to storage modulus) can be associated with the α transition or glass transition temperature [77]. The corresponding peak can be rationalized to the segmental chain mobility and increased degree of freedom due to the conformational arrangement of the polymer chain. It is essential to mention here that the enhanced glass transition temperature for fiber-reinforced composite (Table 2) in both the testing mode cannot be substantiated to just polycarbonate of the composite. Although the shift in glass to rubbery transition temperature for composite emerged, due to the restricted segmental motion polycarbonate in aramid fiber as per the concept of glass transition temperature as isoviscous state [51]. We postulated that the diminishing peak height of Tan δ can be contemplated to the improved working temperature since high Tan δ values demonstrate non-reversible structural deformation in the polymeric system [64].

The dynamic mechanical response from polymeric materials involves physical change as a function of temperature, while the thermal or heat effect can be exemplified via differential scanning calorimetry (DSC) and temperature modulated DSC [63]. DSC is one of the most accepted methodologies to measure the heat flow in the polymer system as the function of temperature and subsequently identifies its glass transition temperature. Höhne et al. have elucidated that during the glass transition temperature, the intrinsic attributes of polymer and measurement variables turned into a time-dependent phenomenon, and system passes through the non-equilibrium

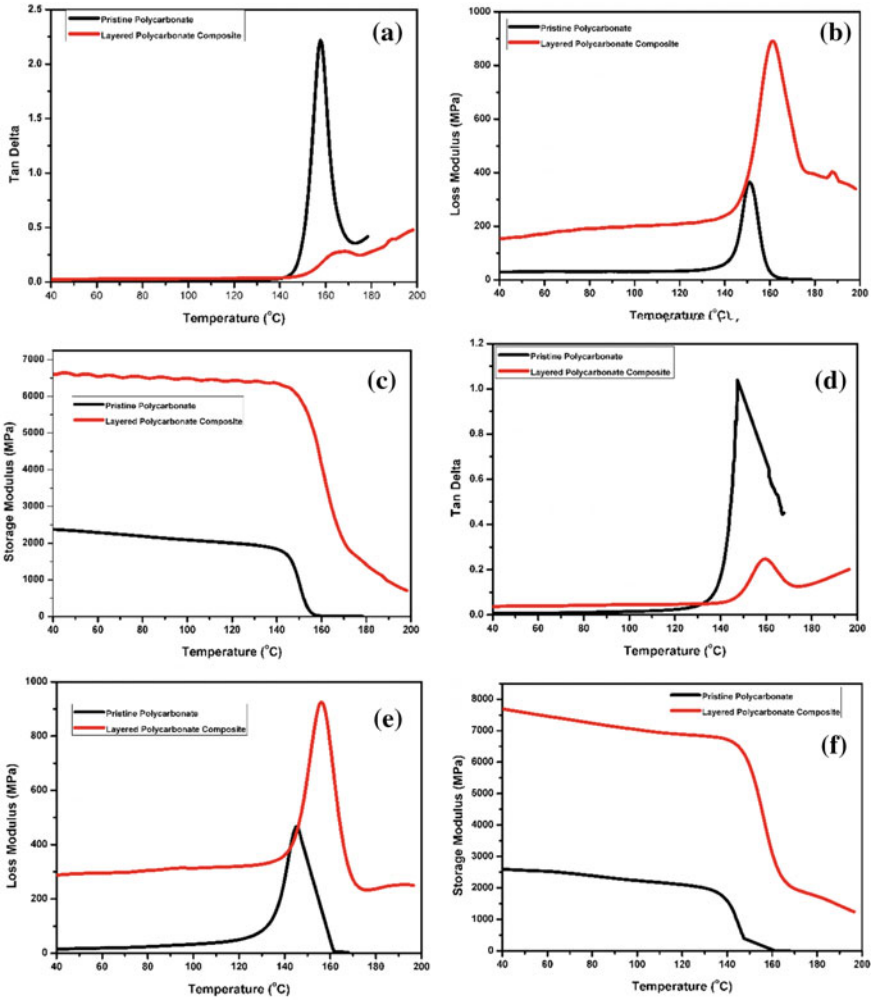

Fig. 4 Dynamic mechanical analysis for pristine polycarbonate and fiber-reinforced composite **a–c** tensile mode of DMA, **d–f** 3-point bend mode

state where classical thermodynamics is not applicable [33]. Therefore, the second-order transition (glass transition) requires heat to pass through that non-equilibrium relaxation stage and subsequently renders step in DSC spectra (circled region in Fig. 5a). Although the evaluation of Tg from the step transition is subjective [63], but in the current study, the onset temperature of the relaxation has been considered as glass transition temperature (Table 3). Since DSC evaluates the combined effect of heat capacity and enthalpic relaxation, therefore, its inadequacy to resolve step transition in some systems curtails its effective utilization, as illustrated in Fig. 5a (for fiber-reinforced PC composite). In this context, temperature modulated DSC

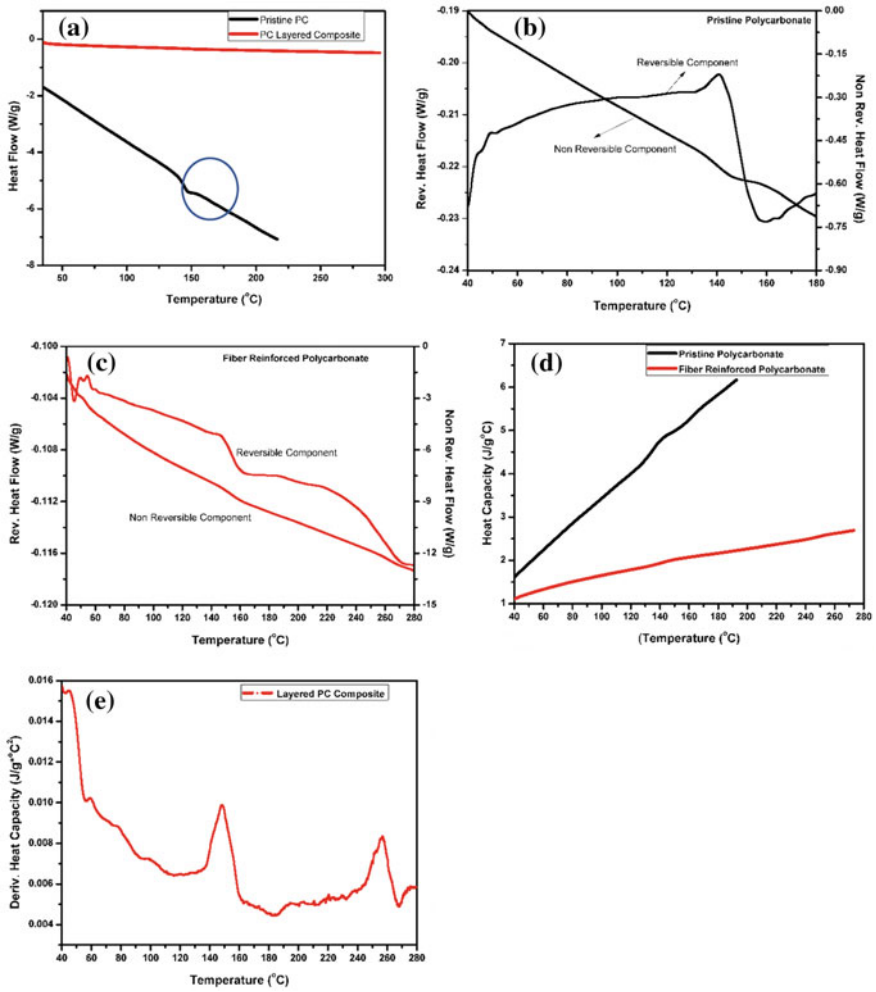

Fig. 5 **a** Differential scanning calorimetry for PC and FRL PC composite, **b** temperature modulated DSC of polycarbonate, **c** temperature modulated DSC of FRL PC composite, **d** heat capacity for PC and FRL PC composite, and **e** derivative heat capacity for FRL PC composite

can provide significant insight by the virtue of its efficacy to measure reversible (heat flow-change of heat capacity with temperature) [58] and non-reversible heat flow (non-reversible heat flow-change of heat capacity with time) [58] separately as discerned in Fig. 5b, c. In addition to rev and non-rev heat flow component, Fig. 5d exhibits the heat capacity difference between the pristine polycarbonate and fiber-reinforced PC composite which can be effectively explained on the basis of fundamental hypothesis related to the heat capacity. The heat capacity of a polymeric system mainly deliberated in two components, i.e., lattice vibration (skeleton vibration: low frequency acoustic vibration) and vibration from internal motion (high

frequency vibration compare to lattice vibration) [30]. The contribution of internal motion to the heat capacity is considerably higher compared to the lattice vibration at the working temperature of the polymer (>100 K) [30]. Such atomic motion in macromolecules involves bond stretching, bond bending, torsional oscillation, flipping of structural unit from one equilibrium to another equilibrium, and cooperative motion [10]. Therefore, any hinderance to the motion of atom or group of atoms largely influences the characteristics of heat capacity. In this context, it can be enumerated that the significant reduction in heat capacity of fiber-reinforced PC composite emerged due to the restricted intermolecular and intramolecular motion of PC in the entire temperature range. Hourston et al. have demonstrated that the temperature derivative of heat capacity can be effectively utilized to illustrate various transitions observed in the temperature modulated DSC [38]. Figure 5e delineates the derivative heat capacity of the fiber-reinforced PC composite, where the first peak of the spectra can be corroborated to the α relaxation of the polymer while the secondary peak corresponds to the melting of the PC matrix.

Thermogravimetric analysis has been considered as another efficient technique other than DSC and temperature modulated DSC to evaluate the thermal stability of the polymeric system and its composite. Thermogravimetric analysis of the pristine polycarbonate and fiber-reinforced PC composite has been delineated in Fig. 6a, b, where Fig. 6a elucidated the loss weight fraction with the function of temperature and Fig. 6b demonstrates the rate of loss of weight fraction (a derivative of mass loss). The degradation mechanism of polycarbonate and aramid fibers has been extensively reported elsewhere [1, 12, 13, 24, 43, 46, 50, 55–57], and therefore the current study

Table 2 Structural stability in terms of temperature (obtained from DMA)

	Pristine polycarbonate (tensile mode)	FRL PC composite (Tensile Mode)	Pristine polycarbonate (3-point mode)	FRL PC composite (3-point mode)
Storage modulus (°C) onset	145.66	153.35	139.51	149.13
Loss modulus (°C) peak position	151.69	161.21	145.76	156.07
Tanδ (°C)peak position	157.74	169.32	147.41	159.22

Table 3 Thermal attributes of polycarbonate and its FRL composites

	Onset temperature of degradation (°C)	Ea (kJ/mol.)	T_{50}	Ea (kJ/mol.)
Pristine polycarbonate	475.56	123.79	515.46	121.38
Aramid fiber	504.51	25.60	533.29	147.40
FRL PC composite	429.27	63.42	551.68	41.57

mainly focused on the evaluation of thermal stability expressed in terms of temperature where 50% (T_{50})of the mass has been lost compared to its final value in inert environment [32]. Fiber-reinforced PC composite has demonstrated the augmentation in thermal stability (T_{50} = 551.68) as elucidated in Table 3. It is evident from Fig. 6b, FRL PC composite exhibits the characteristics of thermal spectra of neither polycarbonate nor aramid fiber. Such stimulating attributes can be predominantly explained by more detailed elemental analysis for detailed contemplation on degradation mechanism, but the activation energy can provide insight into the thermal stability in addition to T_{50}. Apparent activation energy from thermogravimetry data can be obtained from linear extrapolation of Arrhenius equation (Eq. 1) assuming degradation process as first-order kinetic with its applicability to the small extent of degradation [22, 78]. The slop of the linear approximation plot of Arrhenius equation discern the apparent activation energy, as demonstrated in Fig. 6c–d and further tabulated in Table 3. It is evident from the table that the available activation energy for FRL PC composite is between the activation energy of pristine polycarbonate and aramid fiber before the onset of the degradation process. Essentially, the decomposition process, by definition, refers to the breaking of materials by physical or chemical means and providing initial alteration in structural characteristics for total degradation to be ensued [42]. The initiation or completion of the decomposition process requires some form of energy, and therefore, if available energy at an instance is comparatively smaller, then the system is gleaned from being thermally stable. In this context, we envisioned that the developed FRL PC composite thermally more stable beyond the onset of degradation phenomenon (475–550 °C) (Fig. 6d) compare to both aramid and pristine PC, but its thermal stability is not comparable to aramid during the onset of decomposition (Fig. 6c).

$$\ln\left[\frac{\ln\frac{w_o}{w}}{t}\right] = \left(-\frac{E_a}{R}\right)\frac{1}{T} + \ln k_o \tag{1}$$

where w_o = initial weight w = weight at the time t (min) E_a = apparent activation energy R = ideal gas constant (8.314 J/K. mol.) T = absolute temperature k_o = Arrhenius constant.

In order to further evaluate the mechanical characteristics of polycarbonate, we have exploited the utilization of the notch impact testing technique followed by high-velocity muzzle impact. It is widely acknowledged that polycarbonate is notch sensitive, and sharpening the notch dimension can transform its ductile fracture attribute to the brittle fracture characteristic [21]. It is obvious from Fig. 7 that polycarbonate in the current study exhibits sufficiently high impact energy, but the fiber reinforcement in PC augmented the impact energy by many folds, and complete fracture along the width was not observed even with the application of 22 J load pendulum. The fracture surface of FRL PC composite has been demonstrated in Fig. 3c, d, which clearly elucidate that fracture phenomenon is significantly eclipsed by fiber splitting and fibril fracture without discerning the failure phenomenon of PC particulate.

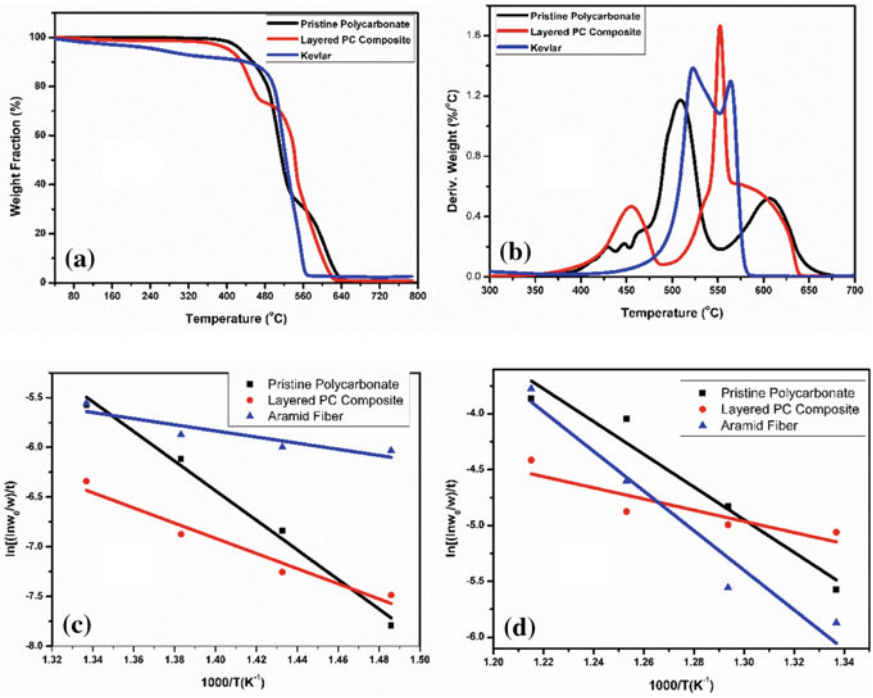

Fig. 6 **a** Thermogravimetric analysis for PC, aramid, and FRL PC composite, **b** derivative weight fraction of PC, aramid, and FRL PC composite, **c** Arrhenius approximation before the onset of degradation, and **d** Arrhenius approximation beyond the onset of degradation

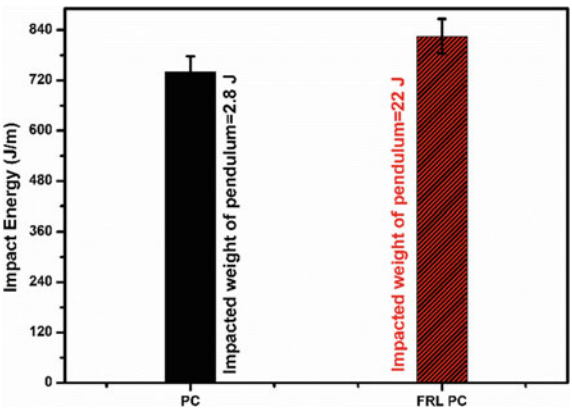

Fig. 7 Elucidation of impact energy for PC and FRL PC composite

Polycarbonate was first instituted for the development of lightweight and transparent protection equipment like safety goggles, industrial machine guards, aircraft windscreen, and police riot shields [52]. Wright et al. have evaluated the perforation and penetration phenomenon in polycarbonate and demonstrated that five main attributes can be realized against the subordinance velocity impact depending on thickness of the sheet or plate, i.e., elastic dishing, deep penetration, cone cracking, and plugging [72, 73]. Edward et al. have further reported that though a wide range of ballistic phenomena was exploited by Wright et al., but the ductile to brittle transition was not effectively discussed [27]. They have performed an experiment on polycarbonate by throwing the materials utilized in riots, i.e., brick (11.7 ± 2.5 m/s), golf ball (24.2 ± 5.3 m/s), and ball bearing (23.2–96.2 m/s). The obtained results were concluded as (i) the velocity achieved by the rioter was found to be lower which do not possess the ability to produce any macroscopic damage to polycarbonate, (ii) at the velocity greater than 50 m/s, the damage become the function of mass and shape of the impacting the projectile. Therefore, the terminal ballistic phenomenon in polycarbonate can be corroborated to the number factor that includes shape of the projectile, thickness of the target, and type of the projectile and velocity of the projectile. Polycarbonate is mainly exploited as ballistic materials in the combination of glass (connected with polyvinyl butyral), which shattered when fired the bullet and retard the projectile enough so that PC prevents the penetration of the projectile [6, 35, 41, 70].

The stimulating characteristics of impact result enticed further to evaluate the developed composite against the high-velocity muzzle impact. As elucidated earlier that high impact velocity on developed composite was performed by 7.62×39 mm steel core projectile with the velocity of 747 ± 15 m/s at the distance of 10 m. Before performing the ballistic impact on the FRL PC composite, an x-ray tomographic scan was carried out to contemplate available defects, as exemplified in Fig. 8a and scanning video provided in supporting information (video V-1) [59]. As ascertained in the figure and video imaging of the composite sample, common laminated composite defects like voids, interlayer, or intralayer delamination and cracks are not visually available [2]. In this context, we have postulated that the developed FRL PC composite is dimensionally and structurally integrated and intact, which was also observed in dynamic mechanical analysis in tension and 3-point bend mode. Later, the analogous tomographic scan was performed after the ballistic impact (Fig. 8b and supporting information video V-2) and the ballistic efficacy was evaluated, based on absorbed energy (calculated as per Eq. 2) [48, 60]. The absorbed energy by the FRL PC composite was observed to be 240.22 J (calculated from Eq. 2) for the velocity range provided in Fig. 8b. The failure phenomenon of polycarbonate [5, 62, 72, 73], and aramid fibers have been extensively reported separately [11, 76] failure phenomenon in the current study requires further deliberation because we did not observe any characteristic fracture features like delamination, interfacial debonding, intra and interlaminar fiber shear or high-temperature localized melting under computed tomographs.

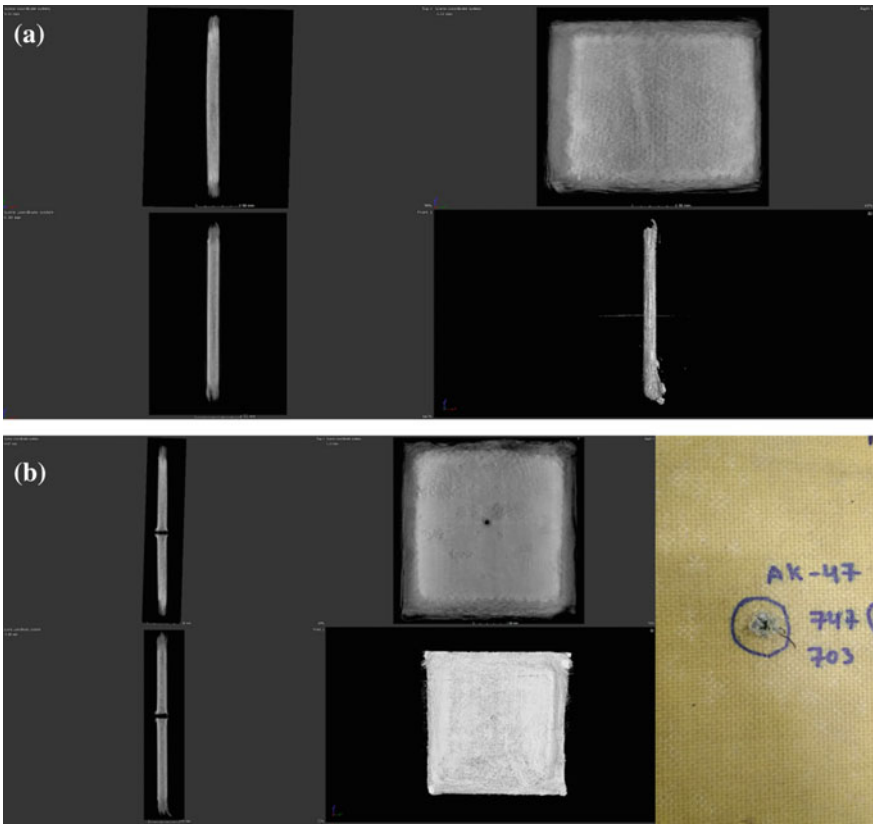

Fig. 8 **a** Computed tomographic image of FRL PC composite before ballistic impact and **b** computed tomographic image after ballistic impact

$$E_{abs} = \frac{1}{2} m_p (V_i^2 - V_r^2) \tag{2}$$

where E_{abs} = energy absorbed by the composite (J);m_p = mass of the projectile (kg);V_i = impacted velocity (m/s); V_r = residual velocity (m/s).

The response of the ballistic materials under low-velocity impact is primarily limited to the elastic range of the materials without any practical damage. Whereas the ordnance velocity (500 to 2000 m/s) impart gross deformation, localized melting and even complete disintegration of impacted materials as observed in the current study [62]. The comprehensive account for temperature variation becomes essential in dynamic conditions (strain rate more than 10^{-2} s) for the distinctive property evaluation of the impacted materials. In the current study, it is believed that the failure phenomenon in developed composite was induced when the structure approached the critical state, and its load capacity diminished. In this view, the dynamic strength of materials is subjugated by the strength at high temperature and pressure in the shocked

state [61]. In the current study, the developed composite demonstrated augmented structural and thermal stability at high temperature, observed from dynamic mechanical analysis and DSC studies. It is envisioned that such high-temperature stability of layered composite essentially contributed to its ballistic performance. Primarily, the ballistic performance of polyaramid fibers depends on the effective distribution of impact energy via a number of factors including yarn pull out, inter and intra-yarn friction, etc. Such phenomenological attributes of polyaramid fiber were not observed under the ballistic impact, therefore, it is believed that thermal characteristics of the composite turned into compelling aspects of the developed composite.

4 Conclusions

The current study explicates the method and its validation in terms of biomimicking the mollusk structure in engineering thermoplastic and high-performance aramid fiber to elucidate the effect of layered architecture on its thermomechanical property. The initial section of the study mainly focused on the thermal property of polycarbonate and its composite under various techniques including DSC, temperature modulated DSC, DMA, and thermogravimetric analysis. The dynamic mechanical analysis and DSC spectra have illustrated significant improvement in thermomechanical property of the FRL PC composite due to the restricted motion of localized atom or group of atoms in addition to the impeded cooperative segmental motion. The insight into the thermal stability was further evaluated by Arrhenius approximation for thermogravimetric analysis, which rendered that the available energy before the onset point is significantly low to trigger the decomposition phenomenon as observed in polycarbonate. The second section of the study involves the mechanical validation of developed composite, which consists of low energy impact (Izod notch test) and high-speed projectile impact. The fracture surface of the developed composite demonstrated the predominance of fiber splitting and fibril fracture as a failure mechanism instead of visible failure characteristics of polycarbonate. It is essential to note that though the current study does not elucidate the detailed ballistic failure phenomenon, we envisioned that the utilized process for mimicking nacreous architecture and stimulated thermomechanical property of the composite to possess the ability to be exploited as high impact material with some further structural deliberation.

Acknowledgements The authors acknowledge Vice-Chancellor, Deakin University, Australia, for their continuous encouragement and support. Authors also acknowledge the assistance provided by Deakin technical staff in performing thermal characterization of the sample. Authors also acknowledge the support from Alex Daniel, ASL DRDO, Government of India and PR Subba Reddy, DRDL DRDO, Government of India for their extensive support in carrying the ballistic as well industrial computed tomographic test.

References

1. Abbås KB (1980) Thermal degradation of bisphenol A polycarbonate. Polymer 21(8):936–940
2. Adams R, Cawley P (1988) A review of defect types and nondestructive testing techniques for composites and bonded joints. NDT International 21(4):208–222
3. Agarwal BD, Broutman LJ, Chandrashekhara K (2017) Analysis and performance of fiber composites, Wiley
4. Aizenberg J, Fratzl P (2009) Biological and biomimetic materials. Adv Mater 21(4):387–388
5. Al-Lafi W, Jin J, Song M (2016) Mechanical response of polycarbonate nanocomposites to high velocity impact. Eur Polymer J 85:354–362
6. Allen G, Morley D, Williams T (1973) The impact strength of polycarbonate. J Mater Sci 8(10):1449–1452
7. Anand A, Harshe R, Joshi M (2013) Resin film infusion: toward structural composites with nanofillers. J Appl Polym Sci 129(3):1618–1624
8. Bandaru AK, Ahmad S, Bhatnagar N (2017) Ballistic performance of hybrid thermoplastic composite armors reinforced with Kevlar and basalt fabrics. Compos a Appl Sci Manuf 97:151–165
9. Bandaru AK, Chavan VV, Ahmad S, Alagirusamy R, Bhatnagar N (2016) Ballistic impact response of Kevlar® reinforced thermoplastic composite armors. Int J Impact Eng 89:1–13
10. Bicerano J (2002) Prediction of polymer properties: cRc Press
11. Briscoe BJ, Motamedi F (1992) The ballistic impact characteristics of aramid fabrics: The influence of interface friction. Wear 158(1):229–247. https://doi.org/10.1016/0043-1648(92)90041-6
12. Brown J, Ennis B (1977) Thermal analysis of Nomex® and Kevlar® fibers. Text Res J 47(1):62–66
13. Cai GM, Yu WD (2011) Study on the thermal degradation of high performance fibers by TG/FTIR and Py-GC/MS. J Therm Anal Calorim 104(2):757–763
14. Carr DJ, Lewis EA, Breeze J (2017) Ballistic threats and body armour design. Military Injury Biomech (pp 5–18), CRC Press
15. Chang I, Lees J (1988) Recent development in thermoplastic composites: a review of matrix systems and processing methods. J Thermoplast Compos Mater 1(3):277–296
16. Cheeseman BA, Bogetti TA (2003a) Ballistic impact into fabric and compliant composite laminates. Compos Struct 61(1):161–173. https://doi.org/10.1016/S0263-8223(03)00029-1
17. Cheeseman BA, Bogetti TA (2003b) Ballistic impact into fabric and compliant composite laminates. Compos Struct 61(1–2):161–173
18. Chen R, Wang C-A, Huang Y, Le H (2008) An efficient biomimetic process for fabrication of artificial nacre with ordered-nanostructure. Mater Sci Eng, C 28(2):218–222
19. Chen X (2016) Advanced fibrous composite materials for ballistic protection, Woodhead Publishing
20. Cheng Q, Wu M, Li M, Jiang L, Tang Z (2013) Ultratough artificial nacre based on conjugated cross-linked graphene oxide. Angew Chem 125(13):3838–3843
21. Cho K, Yang J, Il B, Chan K, Park E (2003) Notch sensitivity of polycarbonate and toughened polycarbonate. J Appl Polym Sci 89(11):3115–3121
22. Corrêa RA, Nunes RC, Lourenco VL (1996) Investigation of the degradation of thermoplastic polyurethane reinforced with short fibres. Polym Degrad Stab 52(3):245–251
23. Council NR, Committee SSS (2008) Inspired by biology: from molecules to materials to machines: National Academies Press
24. Davis A., Golden J (1968) Thermal degradation of polycarbonate. J Chem Soc B: Phys Organic, pp 45–47
25. Dogan A, Arikan V (2017) Low-velocity impact response of E-glass reinforced thermoset and thermoplastic based sandwich composites. Compos B Eng 127:63–69
26. Eagles DB, Blumentritt BF, Cooper SL (1976) Interfacial properties of kevlar-49 fiber-reinforced thermoplastics. J Appl Polym Sci 20(2):435–448

27. Edwards M, Waterfall H (2008) Mechanical and ballistic properties of polycarbonate apposite to riot shield applications. Plast, Rubber Compos 37(1):1–6
28. El-Shekeil Y, Sapuan S, Abdan K, Zainudin E (2012) Influence of fiber content on the mechanical and thermal properties of Kenaf fiber reinforced thermoplastic polyurethane composites. Mater Des 40:299–303
29. Gilbert M (2016) Brydson's Plastics Materials, William Andrew
30. Godovsky YK (2012) Thermophysical properties of polymers, Springer Science and Business Media
31. Gore PM, Kandasubramanian B (2018) Functionalized Aramid Fibers and Composites for Protective Applications: A Review. Ind Eng Chem Res 57(49):16537–16563
32. Groenewoud WM (2001) Thermogravimetrical analysis characterisation of polymers by thermal analysis, pp 60–75, Elsevier
33. Günther H, Wolfgang FH, Flammersheim H-J (2003) Differential Scanning Calorimetry. Springer-Verlag, Berlin Heidelberg, Germany
34. Hare P (1965) Amino acid composition of some calcified proteins. Carnegie Inst Washington Yearbk. 64:223–232
35. Hazell P, Edwards M, Longstaff H, Erskine J (2009) Penetration of a glass-faced transparent elastomeric resin by a lead–antimony-cored bullet. Int J Impact Eng 36(1):147–153
36. Hearle JW (2001) High-performance fibres, Elsevier
37. Heijboer J (1965) Physics of non-crystalline solids. JA Prins 231
38. Hourston DJ, Song M, Pollock HM, Hammiche A (1997) Modulated differential scanning calorimetry. J Therm Anal 49(1):209–218. https://doi.org/10.1007/bf01987441
39. Hudgin D, Bendler T (2000) Handbook of polycarbonate science and technology: Marcel Dekker, New York
40. Illers K, Breuer H, Kolloid Z, (1961) CrossRefl Web of Science® Times Cited, 125, 176, 110
41. Illinger JL, Lewis RW, Barr DB (1975) Effects of adhesive structure on impact resistance and optical properties of acrylic/polycarbonate laminates. Adhesion Sci Technol pp 217–232, Springer
42. Iyer R, Vijayan K (1999) Decomposition behaviour of Kevlar 49 fibres: Part I. AtT≈ T d. Bull Mater Sci 22(7):1013–1023
43. Jang BN, Wilkie CA (2004) A TGA/FTIR and mass spectral study on the thermal degradation of bisphenol A polycarbonate. Polym Degrad Stab 86(3):419–430
44. Kluin J, Yu Z, Vleeshouwers S, McGervey J, Jamieson A, Simha R (1992) Temperature and time dependence of free volume in bisphenol A polycarbonate studied by positron lifetime spectroscopy. Macromolecules 25(19):5089–5093
45. Kulkarni S, Gao X-L, Horner S, Zheng J, David N (2013) Ballistic helmets–their design, materials, and performance against traumatic brain injury. Compos Struct 101:313–331
46. Lee LH (1964) Mechanisms of thermal degradation of phenolic condensation polymers. I. Studies on the thermal stability of polycarbonate. J Polym Sci Part A General Papers 2(6):2859–2873
47. Lee SM (1989) International encyclopedia of composites, VCH
48. Lee YS, Wetzel ED, Wagner NJ (2003) The ballistic impact characteristics of Kevlar® woven fabrics impregnated with a colloidal shear thickening fluid. J Mater Sci 38(13):2825–2833
49. Li H, Ding F, Wang G, Zhang J, Bian X (2001) Evolution of small nickel cluster during solidification. Solid State Commun 120(1):41–46
50. Li XG, Huang MR (1999) Thermal degradation of Kevlar fiber by high-resolution thermogravimetry. J Appl Polym Sci 71(4):565–571
51. Lipatov Y (1978) The iso-free-volume state and glass transitions in amorphous polymers. Polymer Chem, pp 63–104, Springer
52. Malcolm CH (2012) Transparent Armour. In: Laible R (ed) Ballistic materials and penetration mechanics, vol 5. Elsevier, New York, pp 116–134
53. Mantia FL, Spadaro G, Acierno D (1981) Moisture effect on dynamic-mechanical and dielectric properties of some polycarbonates. Acta Polym 32(4):209–211

54. Matsuoka, S, Ishida Y (1966) Multiple transitions in polycarbonate. J Polym Sci Part C: Polymer Symposia 247–259
55. McNeill I, Rincon A (1991) Degradation studies of some polyesters and polycarbonates—8. Bisphenol A polycarbonate. Polymer Degradation and Stability, 31(2):163–180
56. McNeill I, Rincon A (1993) Thermal degradation of polycarbonates: reaction conditions and reaction mechanisms. Polym Degrad Stab 39(1):13–19
57. Mosquera ME, Jamond M, Martinez-Alonso A, Tascon JM (1994) Thermal transformations of Kevlar aramid fibers during pyrolysis: infrared and thermal analysis studies. Chem Mater 6(11):1918–1924
58. Reading M, Hourston DJ (2006) Modulated temperature differential scanning calorimetry: theoretical and practical applications in polymer characterisation (vol 6), Springer Science and Business Media.
59. Reddy M, Lukose S, Subramanian M, Rao G, Muralidhar C, Balasubramaniam K (2011) Industrial computed tomography system for aerospace applications: development and characterisation. Insight-Non-Destructive Testing and Condition Monitoring 53(6):307–311
60. Reddy PRS, Reddy TS, Madhu V, Gogia A, Rao KV (2015) Behavior of E-glass composite laminates under ballistic impact. Mater Des 84:79–86
61. Rosenberg Z, Dekel E (2012) Terminal ballistics, Springer
62. Rosenberg Z, Kositski R (2017) Deep indentation and terminal ballistics of polycarbonate. Int J Impact Eng 103:225–230
63. Saldivar-Guerra E, Vivaldo-Lima E (2013) Handbook of polymer synthesis, characterization, and processing. Wiley
64. Sepe M (1998) Dynamic mechanical analysis for plastics engineering: William Andrew.
65. Sun J, Bhushan B (2012) Hierarchical structure and mechanical properties of nacre: a review. RSC Adv 2(20):7617–7632
66. Tang Z, Kotov NA, Magonov S, Ozturk B (2003) Nanostructured artificial nacre. Nat Mater 2(6):413
67. Tanner D, Fitzgerald JA, Phillips BR (1989) The kevlar story—an advanced materials case study. Angew Chem, Int Ed Engl 28(5):649–654
68. Thomason J, Vlug M (1997) Influence of fibre length and concentration on the properties of glass fibre-reinforced polypropylene: 4. Impact properties. Composites Part A: Appl Sci Manuf 28(3):277–288.
69. Vieille B, Casado VM, Bouvet C (2013) About the impact behavior of woven-ply carbon fiber-reinforced thermoplastic-and thermosetting-composites: a comparative study. Compos Struct 101:9–21
70. Walley S, Field J, Blair P, Milford A (2004) The effect of temperature on the impact behaviour of glass/polycarbonate laminates. Int J Impact Eng 30(1):31–53
71. Wang J, Cheng Q, Tang Z (2012) Layered nanocomposites inspired by the structure and mechanical properties of nacre. Chem Soc Rev 41(3):1111–1129
72. Wright S, Fleck N, Stronge W (1993a) Ballistic impact of polycarbonate-an experimental investigation. Int J Impact Eng 13(1):1–20
73. Wright SC, Fleck NA, Stronge WJ (1993b) Ballistic impact of polycarbonate—an experimental investigation. Int J Impact Eng 13(1):1–20. https://doi.org/10.1016/0734-743X(93)90105-G
74. Wyzgoski MG, Yeh GS-Y (1973) Relation between free volume and the low-temperature "Beta" Transition in Glassy Polycarbonate. Polym J 4(1):29
75. Yadav R, Goud R, Dutta A, Wang X, Naebe M, Kandasubramanian B (2018) Biomimicking of Hierarchal Molluscan Shell Structure Via Layer by Layer 3D Printing. Ind Eng Chem Res 57(32):10832–10840. https://doi.org/10.1021/acs.iecr.8b01738
76. Yadav R, Naebe M, Wang X, Kandasubramanian B (2016) Body armour materials: from steel to contemporary biomimetic systems. RSC Advances 6(116):115145–115174
77. Yadav R, Naebe M, Wang X, Kandasubramanian B (2017) Structural and Thermal Stability of Polycarbonate Decorated Fumed Silica Nanocomposite via Thermomechanical Analysis and In-situ Temperature Assisted SAXS. Scientific Reports 7(1):7706

78. Yang W, Macosko C, Wellinghoff S (1986) Thermal degradation of urethanes based on 4, 4′-diphenylmethane diisocyanate and 1, 4-butanediol (MDI/BDO). Polymer 27(8):1235–1240
79. Yao HB, Tan ZH, Fang HY, Yu SH (2010) Artificial Nacre-like Bionanocomposite Films from the Self-Assembly of Chitosan-Montmorillonite Hybrid Building Blocks. Angew Chem Int Ed 49(52):10127–10131
80. Yee A, Smith S (1981) Molecular structure effects on the dynamic mechanical spectra of polycarbonates. Macromolecules 14(1):54–64
81. Zhang Y, Gong S, Zhang Q, Ming P, Wan S, Peng J, Cheng Q (2016) Graphene-based artificial nacre nanocomposites. Chem Soc Rev 45(9):2378–2395